PNAS
www.pnas.org

Supplementary Information for

Active unfolding of the Glucocorticoid Receptor by the Hsp70/Hsp40 chaperone system in single-molecule mechanical experiments

Patrick Moessmer [1], Thomas Suren [1], Ulrike Majdic [1], Vinay Dahiya [2], Daniel Rutz [2], Johannes Buchner [2], Matthias Rief [1,*]

[1]Center for Protein Assemblies and Department Physik E22, Technical University Munich, 85748 Garching, Germany

[2]Center for Protein Assemblies and Department Chemie, Technical University Munich, 85748 Garching, Germany

[*]Corresponding author

Contact of corresponding author:
Matthias Rief
Email: matthias.rief@mytum.de

This PDF file includes:

Supplementary text
Figures S1 to S4
Table S1

Materials and Methods

Biochemical Methods:

All protein constructs were prepared using standard recombinant techniques described below. The experiments were carried out using the custom-built dual-beam optical tweezers described in (1). Wormlike-chain fitting was conducted as described in SI (equations S1 and S2). Hidden Markov Model (HMM) based assignment of states was performed as in (2).

Protein expression and sequences:

GR-LBD:

UniProt-P04150 (residues: 521-777)

Protein expression:

Human GR-LBD variants (aa 527-777) were expressed in BL21 (DE3 RIPL) cells at 18°C overnight in ZYM-5052 auto-induction media supplied with 500 µM Dexamethasone (DEX) (Sigma-Aldrich, St. Louis, USA). Cells were harvested by centrifugation for 15 min at 7,000 rpm and 4°C (Beckman Avanti J-26 XP, Beckman Coulter, Brea, California) and washed with ice-cold PBS. Cells were resuspended in Ni-A buffer (50mM Tris, 2 M Urea, 100mM NaCl, 5mM MgCl2, 10mM Imidazole, 2mM ß-mercaptoethanol, 50 µM DEX, pH 7.9) supplemented with DNaseI (Roche, Basel, Swiss) and Protease Inhibitor HP (Serva electrophoresis GmbH, Heidelberg, Germany). Cell suspension was lysed by sonication (Bandelin Sonoplus UW2200, Bandelin electronic, Berlin Germany) or french press (Constant Systems Limited, Low March, UK) and centrifuged for 1 hour at 20,000 rpm and 4°C. Cleared lysate was applied onto a Ni-column (5 ml FF,GE Healthcare, Chalfont St. Giles, Great Britain), pre-equilibrated in Ni-B buffer (50mM Tris, 500mM NaCl, 10mM Imidazole, 10% Glycerol, 2mM ß-mercaptoethanol, 50 µM DEX pH 7.9). The column was then gradient-equilibrated in Ni-B buffer and His6-Halo-GR-LBD was eluted with Ni-C buffer (50mM Tris, 500mM NaCl, 350mM Imidazole, 10% Glycerol, 2mM ß-mercaptoethanol, 50 µM DEX pH 7.9). IMAC-Buffers for the purification of apo-GR-LBD were supplied with 2 mM ATP to prevent binding of *E. coli* GroE and DnaK. GR-protein containing fractions were pooled, supplemented with His6-tagged TEV protease and dialyzed against 50mM Tris, 100mM NaCl, 10% Glycerol, 2mM ß-mercaptoethanol, 0.5% CHAPS, 50 µM DEX pH 7.9 overnight. Then, digested protein was passed through a Ni-column to remove Halo-tag-Fusion and TEV protease. The flow through was concentrated and loaded onto a gel filtration column (Superdex 200, 16/60 pg, GE Healthcare, Chalfont St. Giles, Great Britain) equilibrated in GR-storage buffer (25mM Tris, 100mM NaCl, 10% Glycerol, 0,5% CHAPS, 2mM DTT, 50 µM DEX pH 7.9). GR-proteins were shock-frozen and analyzed by SDS-PAGE.

Sequence:

N-SACK-GR-LBD F602S/C638D-KCL-C ($GRSD$):
SACKQLTPTLVSLLEVIEPEVLYAGYDSSVPDSTWRIMTTLNMLGGRQVIAAVK
WAKAIPGFRNLHLDDQMTLLQYSWMSLMAFALGWRSYRQSSANLLCFAPDLII
NEQRMTLPDMYDQCKHMLYVSSELHRLQVSYEEYLCMKTLLLLSSVPKDGLKS
QELFDEIRMTYIKELGKAIVKREGNSSQNWQRFYQLTKLLDSMHEVVENLLNYC
FQTFLDKTMSIEFPEMLAEIITNQIPKYSNGNIK KLLFHQKCL

Ydj1

UniProt-P25491

Protein expression:

Ydj1 with a cleavable solubility tag (SUMO)was expressed in BL21 (DE3 RIPL) cells, grown in LB with antibiotic selection (kanamycin) to an optical density of 0.7, by induction with 1mM IPTG. After overnight growth at 30°C, cells were harvested by centrifugation for 15 min at 4,600 rpm and 4°C (Centrifuge Rotanta 460R Hettich Zentrifugen, Tuttlingen) and resuspended in Ni-buffer A (40mM HEPES, 150mM KCl, 350mM NaCl, 20mM MgCl2, 5% Glycerol, 10mM Imidazole, 1mM DTT pH 7.5) supplemented with DNaseI (Roche, Basel, Swiss) and Protease Inhibitor AEBSF-HCl (Serva electrophoresis GmbH, Heidelberg, Germany). Cell suspension was lysed by high pressure (Celldisruptor CF1m LTD, Constant Systems, Daventry Northants, United Kingdom) and centrifuged for 1 hour at 38,000 rpm and 4°C. Cleared lysate was applied onto a Ni-column (5 ml FF, GE Healthcare, Chalfont St. Giles, Great Britain), pre-equilibrated in Ni-buffer A. After washing with Ni-buffer A and 6% Ni-buffer B (40mM HEPES, 150mM KCl, 350mM NaCl, 20mM MgCl2, 5% Glycerol, 300mM Imidazole, 1mM DTT pH 7.5) the protein was eluted in 100% Ni-buffer B. Ydj1 containing fractions were pooled and 1:4 diluted with ice-cooled H2O. The solution was supplemented with DTT (1mM) and His6-tagged SENP2 protease and dialyzed against GF-buffer (40mM HEPES, 150mM KCl, 5mM MgCl2 pH7.5) overnight. Digested protein was passed through a Ni-column to remove SUMO-tag-Fusion and SENP2 protease. The flow through

was concentrated and loaded onto a gel filtration column (Superdex 200 **Increase 10/300 GL**, Sigma-Aldrich, St. Louis, U.S.A) equilibrated in GF-buffer. Ydj1-proteins were shock frozen and analyzed by SDS-PAGE.

Sequence:

MVKETKFYDILGVPVTATDVEIKKAYRKCALKYHPDKNPSEEAAEKFKEASAAY
EILSDPEKRDIYDQFGEDGLSGAGGAGGFPGGGFGFGDDIFSQFFGAGGAQR
PRGPQRGKDIKHEISASLEELYKGRTAKLALNKQILCKECEGRGGKKGAVKKCT
SCNGQGIKFVTRQMGPMIQRFQTECDVCHGTGDIIDPKDRCKSCNGKKVENER
KILEVHVEPGMKDGQRIVFKGEADQAPDVIPGDVVFIVSERPHKSFKRDGDDLV
YEAEIDLLTAIAGGEFALEHVSGDWLKVGIVPGEVIAPGMRKVIEGKGMPIPKYG
GYGNLIIKFTIKFPENHFTSEENLKKLEEILPPRIVPAIPKKATVDECVLADFDPAK
YNRTRASRGGANYDSDEEEQGGEGVQCASQ

<u>Human Hsp70:</u>

UniProt-P0DMV8

Protein expression:

Expressed and purified as described for Ydj1.

Sequence:

MAKAAAIGIDLGTTYSCVGVFQHGKVEIIANDQGNRTTPSYVAFTDTERLIGDAA
KNQVALNPQNTVFDAKRLIGRKFGDPVVQSDMKHWPFQVINDGDKPKVQVSY
KGETKAFYPEEISSMVLTKMKEIAEAYLGYPVTNAVITVPAYFNDSQRQATKDA
GVIAGLNVLRIINEPTAAAIAYGLDRTGKGERNVLIFDLGGGTFDVSILTIDDGIFE
VKATAGDTHLGGEDFDNRLVNHFVEEFKRKHKKDISQNKRAVRRLRTACERAK
RTLSSSTQASLEIDSLFEGIDFYTSITRARFEELCSDLFRSTLEPVEKALRDAKLD
KAQIHDLVLVGGSTRIPKVQKLLQDFFNGRDLNKSINPDEAVAYGAAVQAAILM
GDKSENVQDLLLLDVAPLSLGLETAGGVMTALIKRNSTIPTKQTQIFTTYSDNQP
GVLIQVYEGERAMTKDNNLLGRFELSGIPPAPRGVPQIEVTFDIDANGILNVTAT
DKSTGKANKITITNDKGRLSKEEIERMVQEAEKYKAEDEVQRERVSAKNALESY
AFNMKSAVEDEGLKGKISEADKKKVLDKCQEVISWLDANTLAEKDEFEHKRKEL
EQVCNPIISGLYQGAGGPGPGGFGAQGPKGGSGSGPTIEEVD

J-Domain:

UniProt-P25491, residues: 1-103

Protein expression:

Expressed and purified as described for Ydj1.

Sequence:

GSMVKETKFYDILGVPVTATDVEIKKAYRKCALKYHPDKNPSEEAAEKFKEASA
AYEILSDPEKRDIYDQFGEDGLSGAGGAGGFPGGGFGFGDDIFSQFFGAGG

Hdj2:

UniProt-P31689

Protein expression:

Expressed and purified as described for Ydj1, with the exception of the composition of Ni-buffer A (40mM NaH2PO4, 500mM NaCl, 20mM Imidazole, 2mM DTT, 10% Glycerol pH 8.0), Ni-buffer B (40mM NaH2PO4, 500mM NaCl, 500mM Imidazole, 2mM DTT, 10% Glycerol pH 8.0) and GF-buffer (40mM HEPES, 150mM KCl, 5mM MgCl2, 1mM DTT, pH 8.0).

Sequence:

MVKETTYYDVLGVKPNATQEELKKAYRKLALKYHPDKNPNEGEKFKQISQAYE
VLSDAKKRELYDKGGEQAIKEGGAGGGFGSPMDIFDMFFGGGGRMQRERRG
KNVVHQLSVTLEDLYNGATRKLALQKNVICDKCEGRGGKKGAVECCPNCRGT
GMQIRIHQIGPGMVQQIQSVCMECQGHGERISPKDRCKSCNGRKIVREKKILEV
HIDKGMKDGQKITFHGEGDQEPGLEPGDIIIVLDQKDHAVFTRRGEDLFMCMDI
QLVEALCGFQKPISTLDNRTIVITSHPGQIVKHGDIKCVLNEGMPIYRRPYEKGRL
IIEFKVNFPENGFLSPDKLSLLEKLLPERKEVEETDEMDQVELVDFDPNQERRR
HYNGEAYEDDEHHPRGGVQCQTS

Preparation of the optical trap measurements:

For tethering the protein to the beads in our optical trap setup, we used a protocol similar to the one described by Cecconi et al. (3). The protein was incubated with 34 bp 3'-maleimide modified oligonucleotides for 2h at room temperature. The desired oligo-protein-oligo construct was then again purified by size exclusion using a Yarra 3u SEC-3000 column, concentrated to about 0.5 µM, shock-frozen and stored in aliquots at -80°C. On each measurement day, the construct was incubated for 1 h on ice with 180 nm long dsDNA handles that could hybridize to the oligonucleotides. Proper construct formation including 2 dsDNA handles was checked on an Agarose gel. At the other end, half of the handles were biotin-modified, while the other half were digoxigenin-modified. The whole construct was incubated 20 min with 1µm-sized streptavidin-coated beads (polysciences,Inc.) before mixing with antidigoxigenin-coated beads. The measurement chambers were made by attaching parafilm (Bemis Company) between two 170 µm-thick coverslips (Carl Roth).
A custom built dual-beam optical trap as in (1) was used to trap the two different kinds of beads, one in the fixed beam and the other one in the mobile beam, which can be moved using a piezo mirror. The construct was tethered between the two beads by bringing the bead surfaces together in close proximity. Data was recorded with a sampling frequency of 30 kHz. The trap stiffness lay between 0.2 pN/nm and 0.35 pN/nm in all measurements.
All measurements were performed at 23°C in 40mM Tris, 150mM NaCl and 1 mM DTT at pH 8.0 with the addition of 0 to 200µM Dexamethasone (DEX, Sigma D1756). An oxygen scavenger system was added consisting of Pyranose Oxidase, Catalase and Glucose as described in (4).

Data Analysis:

Modeling polymer elasticity in stretch and relax cycles.

The force-extension curves for stretching of the DNA only were modeled by the extensible worm-like-chain (eWLC) model:

$$F_{eWLC}(x) = \frac{k_B T}{p_{DNA}} \left(\frac{1}{4} \left(1 - \frac{x}{L_{DNA}} + \frac{F}{K} \right)^{-2} - \frac{1}{4} + \frac{x}{L_{DNA}} - \frac{F}{K} \right) \qquad \text{[S1]}$$

where $k_B T$ is the thermal energy, p_{DNA} the DNA persistence length, L_{DNA} the DNA contour length and K the elastic stretch modulus.

The force-extension for the unfolded protein part can be similarly described by

$$F_{WLC}(x) = \frac{k_B T}{p_P} \left(\frac{1}{4} \left(1 - \frac{x}{L_P} \right)^{-2} - \frac{1}{4} + \frac{x}{L_P} \right) \qquad \text{[S2]}$$

where p_P is the protein persistence length and L_P the protein contour length.

To fit the curve after part of the protein has unfolded, a linear combination of the two has been applied. We used a fixed p_P of 0.7 nm.

Contour length transformation

The measured forces could be transformed into contour length by inverting eq. S1 and S2, using the elastic properties determined by the stretch and relax cycles before or after the passive-mode experiments (5).

SI Figure 1:

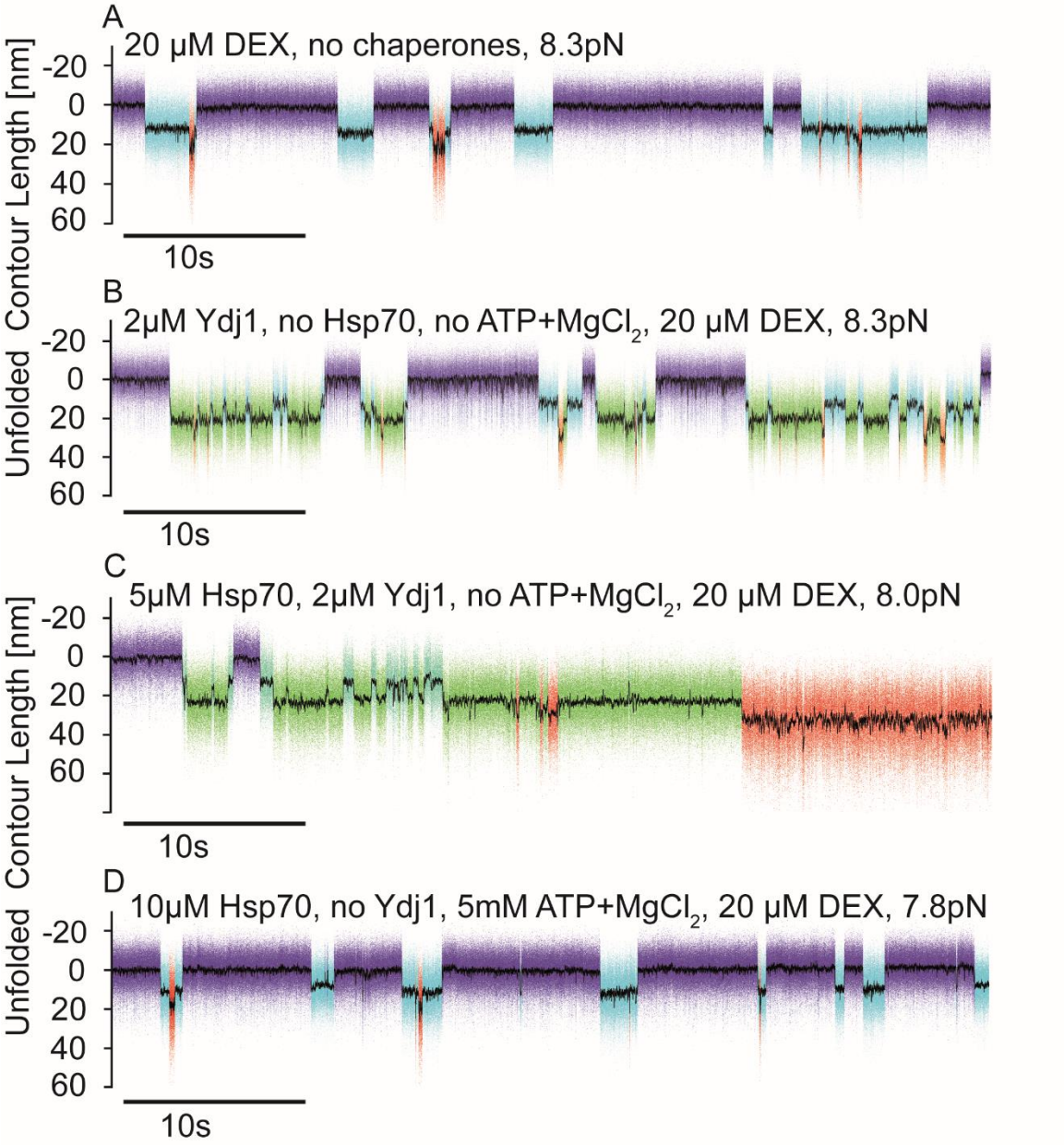

SI Figure 1: **Omission of any one component of the full Hsp70/40 chaperone system leads to no or only partial unfolding.**

A) For comparison, a passive-mode trace of GR-LBD in the absence of chaperones is shown, exhibiting flipping (purple/dark blue transitions), DEX dissociation (light blue) and DEX rebinding (return to purple/dark blue transitions) as well as rare partial unfoldings (red) (5). **B)** At 2µM Ydj1, no Hsp70 and no MgATP, Ydj1 transiently binds to apo GR-LBD at ~20 nm unfolded contour length from the N-terminus. No chaperone-induced unfolding as in the case of the full

Hsp70/40 chaperone system occurs with Ydj1 only. **C)** At 1µM Hsp70, 2µM Ydj1 and no MgATP, the GR-LBD undergoes a very slow and only partial unfolding, which typically stops between 30 and 40nm unfolded contour length. No complete unfolding was observed. Addition of 5mM MgATP would result in fast and complete unfolding within the first 5s after DEX dissociation, as depicted in Fig. 1B. **D)** At 10µM Hsp70 and 5mM ATP, but without Hsp40, the GR-LBD shows the same behavior as in the absence of chaperones (6). No chaperone-induced unfolding happens at these conditions

SI Figure 2:

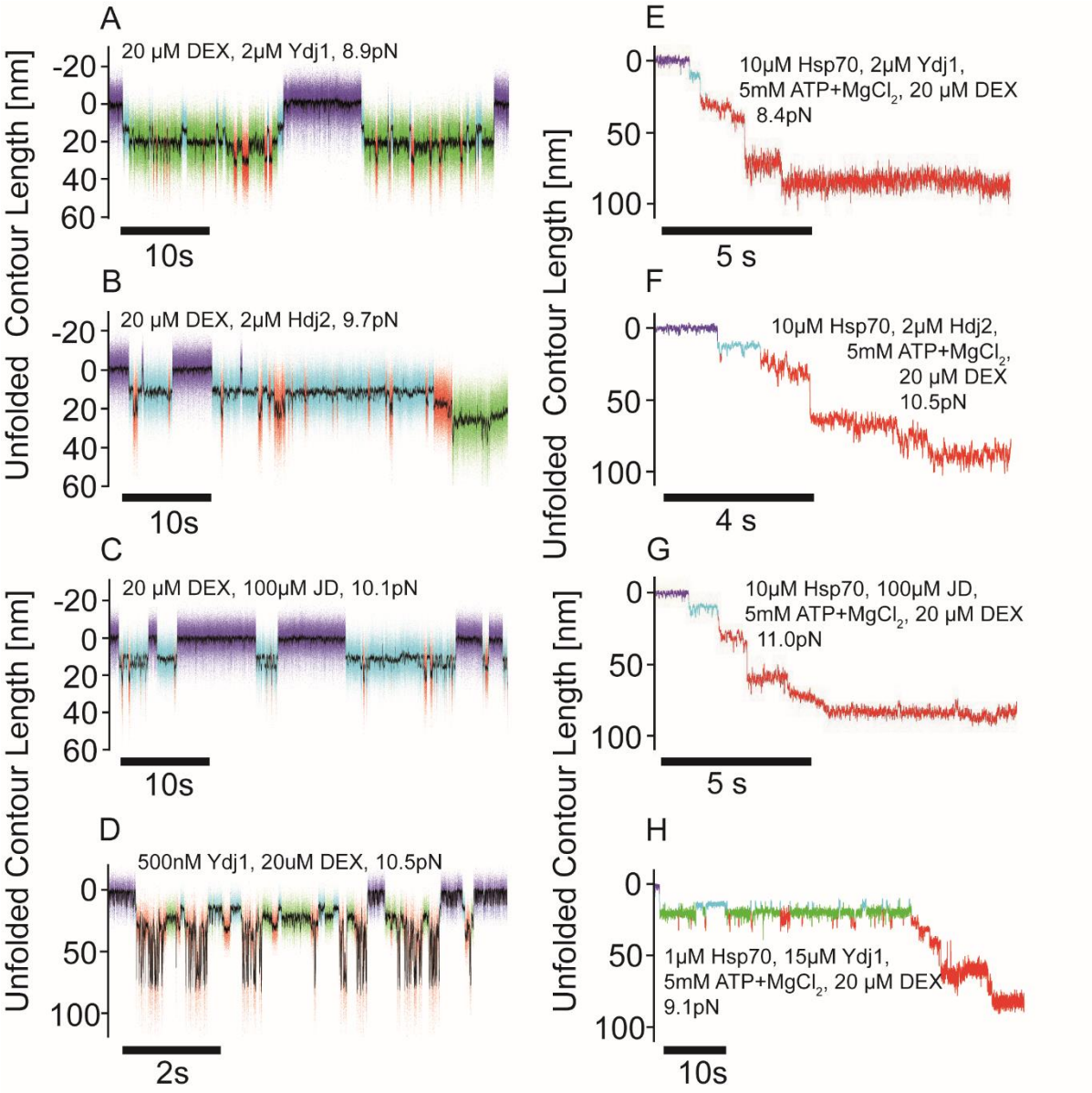

SI Figure 2: The effect of three different variants of the Hsp40 co-chaperone (Ydj1, Hdj2, JD) on GR-LBD with and without Hsp70.

A) Passive-mode trace of GR-LBD in the presence of 500nM Ydj1. A Ydj1 bound state (green) at ~20 nm unfolded contour length from the N-terminus is observed. Binding of Ydj1 is transient and only happens to the DEX-unbound apo state of GR-LBD (transitions to green state only from light blue state). Binding of Ydj1 and DEX to ligand unbound state is competitive (DEX rebinding, i.e. return to purple/dark blue flipping, only occurs from light blue state, never from green state). **B)** Passive-mode trace of GR-LBD in the presence of 2µM Hdj2 (human

homologue of Ydj1). GR-LBD behaved significantly different in the presence of Hdj2 as compared to Ydj1 (A)). In the presence of Hdj2, after a few DEX dissociations and rebindings, GR-LBD is trapped in a partially unfolded state, which it never recovers from (green). Higher Hdj2 concentrations (> 10µM) induce this state usually directly after the first DEX dissociation. Addition of Ydj1 never lead to a comparable irreversibly unfolded state. **C)** Passive-mode trace of GR-LBD in the presence of 100µM J-Domain (truncated Ydj1 construct, JD). In the presence of JD, the GR-LBD behaves exactly the same way as it does in the absence of chaperones (SI Fig. 1A). No effect of JD could be detected. **D)** Ydj1 binding to GR-LBD (green state at ~20nm contour length) at a high force of 10.5pN. The GR-LBD undergoes unfoldings to the completely unfolded state and refoldings back to the native holo state in equilibrium. The only binding of Ydj1 detected in our experiments is the green state at ~20nm contour length. The red further unfolded intermediates show no binding of Ydj1 and the same kinetics as in the absence of Ydj1 (cf. Fig. 3A in main text) **E)** Complete and irreversible unfolding of GR-LBD at 10µM Hsp70, 2µM Ydj1, 5mM MgATP **F)** Complete and irreversible unfolding of GR-LBD at 10µM Hsp70, 2µM Hdj2, 5mM MgATP **G)** Complete and irreversible unfolding of GR-LBD at 10µM Hsp70, 100µM JD, 5mM MgATP **H)** At lower Ydj1 concentrations, Hsp70/40 induced unfolding (red phase at the end of the trace) begin within ~the first 2s after DEX dissociation (cf. Fig. 1 B), SI Fig. 2 E, F, G). However, at 15 µM Ydj1, Hsp70/40 induced unfolding is delayed significantly (~30 s in the trace shown) by Ydj1 binding (green state).

SI Figure 3:

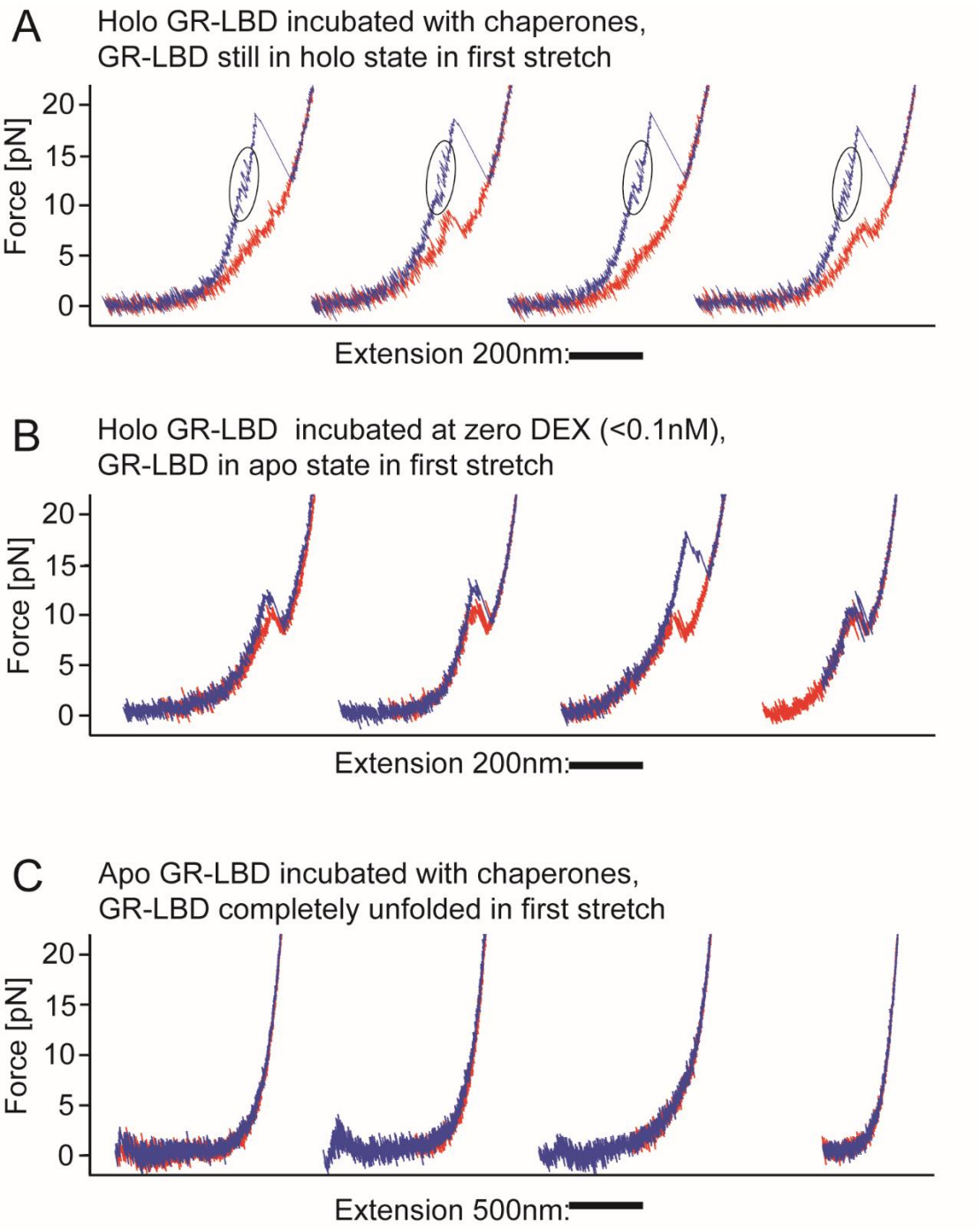

SI Figure 3: Hsp70/40-induced unfolding of GR-LBD works at zero force.

A) First stretch/relax cycle of 4 different GR-LBD molecules showing initial unfolding of holo GR-LBD after incubation at high chaperone concentrations (10

µM Hsp70, 2 µM Ydj1, 5 mM MgATP) for 2h. GR-LBD is always natively folded and DEX bound in the first stretch (holo state), indicating that the chaperones could not attack or unfold holo GR-LBD during the incubation. **B)** First stretch/relax cycle of 4 different GR-LBD molecules showing initial unfolding of apo GR-LBD. Apo GR-LBD was obtained from holo GR-LBD by removing DEX to a final concentration <0.1 nM by buffer dilution and subsequent over-night incubation. GR-LBD was always in the apo state in the first stretch cycle, showing that DEX had dissociated overnight. **C)** First stretch/relax cycle of 4 different GR-LBD molecules showing that, after incubation of apo GR-LBD at high chaperone concentrations (same as in Fig. 3A, 10 µM Hsp70, 2 µM Ydj1, 5 mM MgATP) for 40 min, GR-LBD is always already completely unfolded before stretching starts. Apparently, chaperones had unfolded apo GR-LBD at zero force during the incubation.

SI Figure 4:

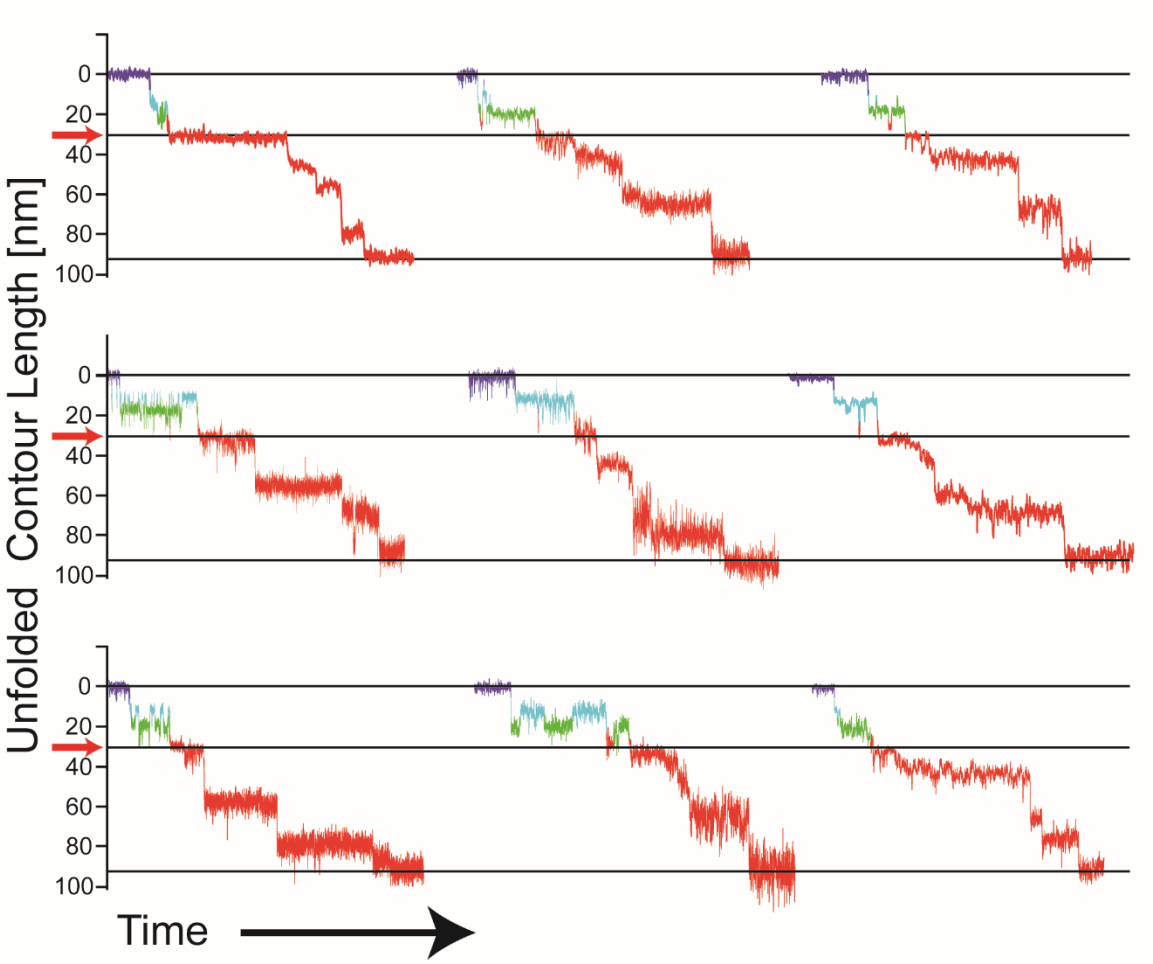

SI Figure 4: **Selected traces, in which the first 32 nm unfolding intermediate is clearly visible.**

All shown traces exhibit the first chaperone-induced unfolding intermediate located at 32nm unfolded contour length from the N-terminus (first red intermediate). The LIMBO algorithm predicts the Hsp70 binding site with the highest binding probability at precisely these 32nm (cf. Fig. 4, (7)). Time scales vary between traces.

SI Table 1:

$k_{on\ Hsp70}$	$0.20 \pm 0.03\ s^{-1}\mu M^{-1}$
$k_{on\ Ydj1}$	$0.78 \pm 0.20\ s^{-1}\mu M^{-1}$
$k_{on\ JD}$	$0.016 \pm 0.004\ s^{-1}\mu M^{-1}$
$k_{\max\ hydrolysis}$	$> 1000\ s^{-1}$

SI Table 1: **Fitting parameters rendered by the global fit to both data sets depicted in Fig. 1F and 1G (variation of Hsp70 while holding Ydj1 constant, and variation of JD while holding Hsp70 constant):**

Our resulting $k_{on\ Hsp70}$ is in the same range as in (8), where they measured $k_{on\ Hsp70} = 0.45\ s^{-1}\mu M^{-1}$. The fact that $k_{on\ Ydj1}$ is ~50-fold higher than $k_{on\ JD}$ is in very good agreement with (9) and (10). Our $k_{\max\ hydrolysis}$ value is to be understood at (hypothetical) infinite chaperone concentrations. It reflects the very small delay between hydrolysis and unfolding transition in our experiments, which must happen almost simultaneously. The highest actually measured unfolding rate in our experiments was $k_{unfold} = 1.34 \pm 0.22\ s^{-1}$, in agreement with previously measured hydrolysis rates ((11) (12)).

SI References:

1. M. Grison, U. Merkel, J. Kostan, K. Djinović-Carugo, M. Rief, α-Actinin/titin interaction: A dynamic and mechanically stable cluster of bonds in the muscle Z-disk. *Proceedings of the National Academy of Sciences* **114**, 1015-1020 (2017).
2. J. Stigler, F. Ziegler, A. Gieseke, J. C. M. Gebhardt, M. Rief, The complex folding network of single calmodulin molecules. *Science* **334**, 512-516 (2011).
3. C. Cecconi, E. A. Shank, F. W. Dahlquist, S. Marqusee, C. Bustamante, Protein-DNA chimeras for single molecule mechanical folding studies with the optical tweezers. *European Biophysics Journal* **37**, 729-738 (2008).
4. M. Swoboda *et al.*, Enzymatic oxygen scavenging for photostability without pH drop in single-molecule experiments. *ACS nano* **6**, 6364-6369 (2012).
5. T. Suren *et al.*, Single-molecule force spectroscopy reveals folding steps associated with hormone binding and activation of the glucocorticoid receptor. *Proceedings of the National Academy of Sciences* **115**, 11688-11693 (2018).
6. R. D. Astumian, M. Bier, Mechanochemical coupling of the motion of molecular motors to ATP hydrolysis. *Biophysical journal* **70**, 637-653 (1996).
7. J. Van Durme *et al.*, Accurate prediction of DnaK-peptide binding via homology modelling and experimental data. *PLoS Comput Biol* **5**, e1000475 (2009).
8. D. Schmid, A. Baici, H. Gehring, P. Christen, Kinetics of molecular chaperone action. *Science* **263**, 971-973 (1994).
9. A. S. Wentink *et al.*, Molecular dissection of amyloid disaggregation by human HSP70. *Nature* **587**, 483-488 (2020).
10. K. Liberek, D. Wall, C. Georgopoulos, The DnaJ chaperone catalytically activates the DnaK chaperone to preferentially bind the sigma 32 heat shock transcriptional regulator. *Proceedings of the National Academy of Sciences* **92**, 6224-6228 (1995).
11. R. Russell, A. W. Karzai, A. F. Mehl, R. McMacken, DnaJ dramatically stimulates ATP hydrolysis by DnaK: insight into targeting of Hsp70 proteins to polypeptide substrates. *Biochemistry* **38**, 4165-4176 (1999).
12. T. Laufen *et al.*, Mechanism of regulation of hsp70 chaperones by DnaJ cochaperones. *Proceedings of the National Academy of Sciences* **96**, 5452-5457 (1999).